ACS APPLIED MATERIALS & INTERFACES

Research Article

www.acsami.org

One-Pot Noninjection Route to CdS Quantum Dots via Hydrothermal Synthesis

Abdelhay Aboulaich,[†,‡] Denis Billaud,[‡] Mouhammad Abyan,[‡] Lavinia Balan,[§] Jean-Jacques Gaumet,[#] Ghouti Medjadhi,[‡] Jaafar Ghanbaja,[‡] and Raphaël Schneider*[,†]

[†]Laboratoire Réactions et Génie des Procédés (LRGP), UPR 3349, Lorraine University, CNRS, 1 rue Grandville, 54001 Nancy Cedex, France

[‡]IJL, Lorraine University, BP 70239, 54506 Vandoeuvre-lès-Nancy Cedex, France

[§]Institut de Science des Matériaux de Mulhouse (IS2M), LRC 7228, 15 rue Jean Starcky, 68093 Mulhouse, France

[#]Laboratoire de Chimie et Physique − Approche Multi-échelle des Milieux Complexes (LCP-A2MC), Lorraine University, ICPM, 1 bd Arago, 57078 Metz Cedex 03, France

Supporting Information

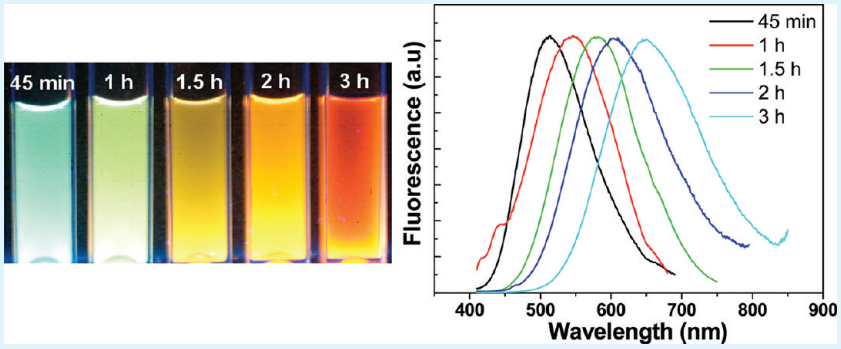

ABSTRACT: Water-dispersible CdS quantum dots (QDs) emitting from 510 to 650 nm were synthesized in a simple one-pot noninjection hydrothermal route using cadmium chloride, thiourea, and 3-mercaptopropionic acid (MPA) as starting materials. All these chemicals were loaded at room temperature in a Teflon sealed tube and the reaction mixture heated at 100 °C. The effects of $CdCl_2$/thiourea/MPA feed molar ratios, pH, and concentrations of precursors affecting the growth of the CdS QDs, was monitored via the temporal evolution of the optical properties of the CdS nanocrystals. High concentration of precursors and high MPA/Cd feed molar ratios were found to lead to an increase in the diameter of the resulting CdS nanocrystals and of the trap state emission of the dots. The combination of moderate pH value, low concentration of precursors and slow growth rate plays the crucial role in the good optical properties of the obtained CdS nanocrystals. The highest photoluminescence achieved for CdS@MPA QDs of average size 3.5 nm was 20%. As prepared colloids show rather narrow particle size distribution, although all reactants were mixed at room temperature. CdS@MPA QDs were characterized by UV−vis and photoluminescence spectroscopy, powder X-ray diffraction, transmission electron microscopy, energy-dispersive X-ray spectrometry and MALDI TOF mass spectrometry. This noninjection one-pot approach features easy handling and large-scale production with excellent synthetic reproducibility. Surface passivation of CdS@MPA cores by a wider bandgap material, ZnS, led to enhanced luminescence intensity. CdS@MPA and CdS/ZnS@MPA QDs exhibit high photochemical stability and hold a good potential to be applied in optoelectronic devices and biological applications.

KEYWORDS: *quantum dots, CdS, hydrothermal synthesis, noninjection, fluorescence, CdS/ZnS core/shell*

INTRODUCTION

Semiconductor quantum dots (QDs) have attracted increasing attention within recent years due to their promising applications in optical devices, solar cells, biosensors, and biological imaging.[1−6] Luminescent QDs present many advantages compared to organic fluorophores such as high photoluminescence (PL) quantum yield (QY), tunable emission wavelength, multiplexing capabilities, and high photostability. Group II−VI semiconductor QDs, especially CdS, CdSe, and CdTe, have been extensively studied because of the ease with which their emission in the visible range can be simply tuned by changing their diameter and the advances in their preparation methods.

Among these materials, CdS is an important direct-band semiconductor with a bandgap (E_g) of 2.42 eV. CdS QDs can be used for photoelectric conversion in solar cells, in light-

Received: February 10, 2012
Accepted: April 17, 2012
Published: April 17, 2012

emitting diodes for flat-panel displays[7−9] and for bioapplications.[10,11] Because the unique properties of QDs are based on diameter, controlling size and size distribution as well as crystallinity and surface defects is crucial. Numerous methods have been developed for the production of CdS QDs. The organometallic approach and its alternatives, based on the high temperature decomposition of organometallic precursors into well-stirred and hot organic solvents, generally provide the best quality QDs.[12−17] However, for many biological applications, the transfer of QDs to water through a capping ligand exchange is necessary. Small thiol-based molecules are generally used to replace hydrophobic capping agents like trioctylphosphine oxide (TOPO) or long-chain amines used to control the growth process at high temperature. In addition, some chemicals used in this route are extremely toxic, pyrophoric and/or expensive. Finally, the organometallic approach is highly unsuitable in terms of scaling up for industrial production because of the high energy requirement of the synthetic process.

In parallel with the success of organic synthetic routes, aqueous routes have also been developed to tackle problems associated with phase transfer. The degradation in optical properties (decrease of PL QY and of photostability) could be avoided by direct synthesis in an aqueous medium. In the aqueous synthesis of CdS QDs, small hydrophilic thiols such as thioglycolic acid (TGA), 3-mercaptopropionic acid (MPA), or thioglycerol (TG) are commonly used as a surface stabilizing agent giving materials with good emission efficiencies.[12,18−23] In both of these methods, nucleation takes place immediately after the injection, and continues until the temperature and the precursor concentration drop below a critical threshold. Because of limitation of the precursor rate and quantity, these methods are not suitable for large-scale preparation of good-quality QDs and are poor in synthetic reproducibility. New synthetic methods that do not require the injection of precursors therefore have to be developed.

A few reports have recently detailed one-pot noninjection routes to semiconductor nanocrystals either via the organometallic method,[24−28] in aqueous solution,[29,30] or under microwave irradiation.[31] In this work, we developed a convenient noninjection one-pot method for the synthesis of good-quality CdS QDs in water by simply mixing $CdCl_2$, thiourea, and 3-mercaptopropionic acid. The synthetic parameters affecting the growth and the optical properties of CdS QDs, such as the Cd/thiourea/MPA ratios, precursor concentrations, pH, and growth temperatures were thoroughly investigated. Highly reproducible large-scale synthesis of CdS QDs with good PL QYs could readily be achieved. The obtained CdS QDs possess high crystallinity, a broad tunable size range, and moderate to good PL QYs (11−20%). The resulting CdS nanocrystals were subsequently overcoated with a ZnS shell (type I QDs) using a mixture of zinc acetate and MPA. During the shell growth, the PL QYs increased to values of 22−23%.

2. EXPERIMENTAL SECTION

2.1. Reagents and Materials. The chemicals used in the experiments included $CdCl_2$. $2.5H_2O$ (99%), 3-mercaptopropionic acid (MPA, 99+%), thiourea (99%), and ethanol (HPLC grade). All chemicals were used without further purification. The 12−14000 molecular weight cut off dialysis membrane tubing (Spectra/Por) was used in the dialysis experiments. All solutions were prepared using Milli-Q water (18.2 MΩ.cm, Millipore) as the solvent.

2.2. Synthesis of MPA-Capped CdS QDs. The Cd^{2+}/thiourea precursors solution was prepared by mixing $CdCl_2$. $2.5H_2O$ (40 mg, 0.175 mmol) and thiourea (22 mg, 0.289 mmol) in 14 mL of ultrapure water. Twenty mL of an aqueous solution of MPA (42 mg, 0.395 mmol) were then added and the pH of the mixture was adjusted to 10 with 1 M NaOH. The typical molar ratio of Cd^{2+}/thiourea/MPA was 1/1.7/2.3 in our experiments. The solution was deaerated with nitrogen-bubbling for 30 min and transferred into a Teflon-lined stainless steel autoclave with a volume of 125 mL. The autoclave was maintained at 100 °C for a designed time and then cooled down to room temperature. Because the reaction vessel was closed, pressure was produced in this system.

2.3. Deposition of a ZnS Shell around CdS@MPA QDs. Ten milliliters of a 0.1 M $Zn(OAc)_2$. $2H_2O$ aqueous solution and 0.35 mL MPA were mixed in a flask. This solution was diluted to 98 mL with water; the pH was adjusted to 10.3 with 4 M NaOH and saturated with N_2 by bubbling for 30 min. Besides this, CdS@MPA nanocrystals were dispersed in water to obtain a Cd concentration of 0.01 mol/L. Thirty mL of the CdS@MPA QDs solution were diluted to 130 mL with water and purged by N_2 for 30 min. Then, 20 mL of the solution of the Zn^{2+}-MPA complex was added dropwise to the diluted CdS QDs solution and the mixture was heated to reflux for 4 h. After cooling to room temperature, the reaction mixture was concentrated to the half using a rotating evaporator (50 °C, 15 mmHg), QDs were precipitated with ethanol and centrifuged. The nanocrystals were further washed with ethanol and finally dried in vacuum at room temperature.

2.4. Dialysis Procedures. Ten milliliters of the unpurified CdS@MPA QDs were placed into the dialysis tubing, and then the solution was dialyzed against ultrapure water for 4 h at room temperature.

2.5. Photostability of CdS and CdS/ZnS QDs. The photostability of aqueous dispersions of CdS and of CdS/ZnS QDs was investigated by irradiating the samples with a 180 mW Hg−Xe lamp under open air condition at room temperature. The distance between the sample solutions and the lamp was fixed to 20 cm. Aliquots of the sample solution were taken out at regular intervals for PL measurements and absorption characterization.

2.6. Instrument. Transmission electron microscopy (TEM) images were taken by placing a drop of the particles in water onto a carbon film-supported copper grid. Samples were studied using a Philips CM20 instrument operating at 200 kV equipped with Energy dispersive X-ray Spectrometer (EDS). Powder (XRD) analyses were obtained using Panalytical X'Pert Pro MPD diffractometre using Cu Kα radiation. Absorption spectra were recorded on a Perkin-Elmer (Lambda 2) UV−visible spectrophotometer. Fluorescence spectra were recorded on a fluorolog-3 spectrofluorimeter *F*222 (Jobin Yvon) using a 450 W xenon lamp. The QY values were determined from the following equation:

$$QY(\text{sample}) = (F_{\text{sample}}/F_{\text{ref}})(A_{\text{ref}}/A_{\text{sample}})(n_{\text{sample}}{}^2/n_{\text{ref}}{}^2)QY_{(\text{ref})}$$

where *F*, *A*, and *n* are the measured fluorescence (area under the emission peak), absorbance at the excitation wavelength and refractive index of the solvent respectively. PL spectra were spectrally corrected and quantum yields were determined relative to Rhodamine 6G in water (QY = 94%).[32]

All mass spectrometry (MS) analyses on CdS QDs were performed on a MALDI coupled to a time-of-flight (MALDI-TOF MS) instrument (Reflex IV, Bruker) operated in positive ion reflectron mode. A 337 nm N_2 laser was used to create ions. The laser energy was set within the range of 30−50% relative to the maximum energy of 1.5 mJ pulse^{-1}. Dithranol was used as the matrix. CdS QDs were dispersed in water mixed with solutions of the matrix, and spotted onto a target plate before laser irradiation. For each sample, at least six mass spectra were recorded to average the measures.

RESULTS AND DISCUSSION

In our approach, the synthesis of CdS QDs involved mixing cadmium chloride, thiourea and 3-mercaptopropionic acid,

followed by heating the reaction mixture in a sealed Teflon tube at 100 °C (Figure 1).

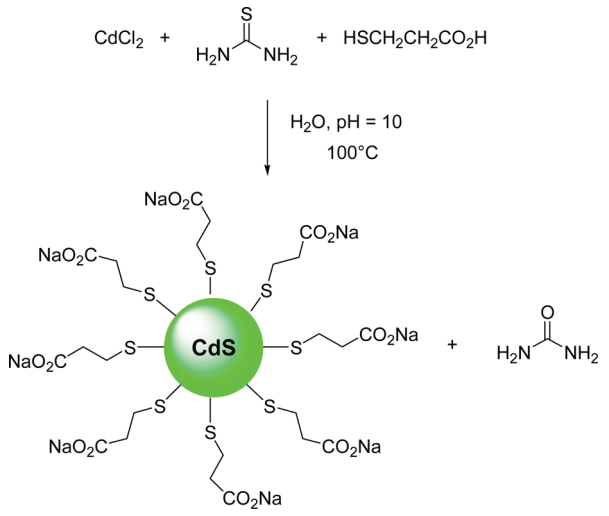

Figure 1. Synthesis of CdS@MPA QDs.

Influence of Experimental Variables. Thiourea was selected as precursor of sulfide ions because its decomposition into sulfide or hydrogenosulfide in water at basic pH has a relatively low activation energy,[33−36] which is favorable for the formation of nuclei and regular QDs. S^{2-} or HS^- anions formed in situ react with the Cd^{2+} salt in the solution to form CdS nuclei that grow by heating to form CdS nanocrystals. The success of our strategy was found to strongly depend on the experimental conditions. Preliminary experiments indicated that CdS QDs could be prepared by using cadmium chloride and a 1.7-fold-excess of thiourea. The samples prepared with more thiourea show a much larger red shift in the PL peak within the same reaction period but their PL QYs were modest (less than 2%). Reactions were conducted at 100 °C in sealed Teflon tubes because lower reaction temperatures were found to favor the formation of nanocrystals with a wider tunable size range.

Figure 2a shows the UV−vis spectra of CdS@MPA QDs prepared using a Cd^{2+}/thiourea/MPA molar ratio of 1/1.7/2.3 and Cd^{2+} concentration of 5 mM after various heating durations (45 min, 1 h, 1.5 h, 2 and 3 h). The absorption edge of bulk CdS is located at 515 nm.[37] Excepted CdS QDs obtained after 3 h heating, all samples showed well-defined first excitonic peaks at respectively 363, 369, 382, 387, and 409 nm, for 45 min, 1, 1.5, 2, and 3 h heating respectively, attributed to $1s_h$-$1s_e$ excitonic transitions.[38] These values indicate that the shift in the absorption peak corresponds to the increase in particle diameter of the CdS QDs with duration of the hydrothermal process. The second, less defined feature at ca. 357 nm could be assigned to the higher spin−orbit component of the 1s−2s transition.[39] The higher energy excitonic transitions are more obvious in the latter samples (the larger particles). The sharp absorption features and the observation of higher energy second excitonic transitions in the absorption spectra are both indicative of monodispersed particles. The variation of the absorption peaks indicates that the particles grow rapidly as the reaction time increased, while the absorption spectrum for the CdS sample (t = 3 h) is broadened. The broadening indicates the onset of conventional

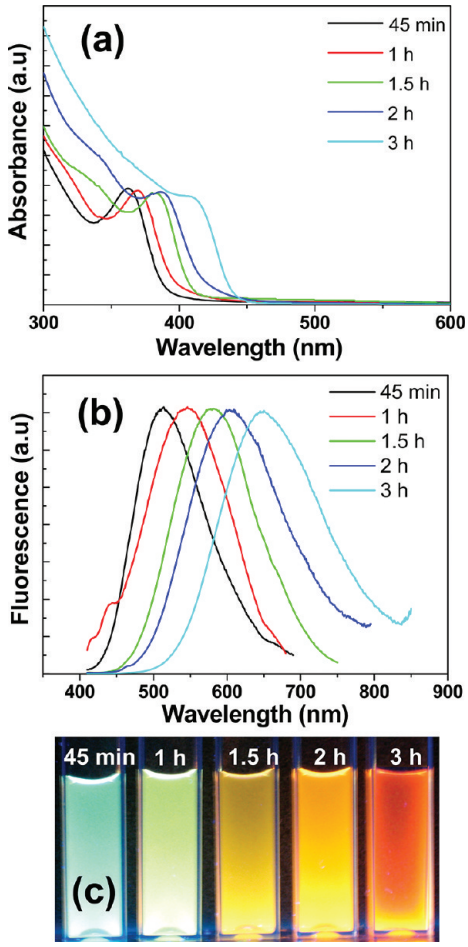

Figure 2. (a) UV−visible and (b) photoluminescence spectra of CdS@MPA QDs after different reaction times at 100 °C, and (c) digital picture of the QDs under UV excitation.

Ostwald ripening, which causes a slow defocusing of the size distribution.[15]

The corresponding absorption edges (obtained by the intersection of the sharply decreasing region of the spectrum with the baseline[40]) are located at 390, 398, 407, 420, and 440 nm for reactions performed during 45 min, 1, 1.5, 2, and 3 h heating, respectively, which corresponds to band gaps of 3.17, 3.11, 3.04, 2.95, and 2.81 eV, respectively. A comparison with the value of bulk CdS having an absorption edge located at 515 nm (2.42 eV) indicates quantum confinement in all prepared nanocrystals. Using these band gap values, the particles diameters were calculated following the formula of Brus based on the effective mass approximation,[41−43]

$$E = E_g + \frac{\hbar^2\pi^2}{2r^2}\left(\frac{1}{m_e} + \frac{1}{m_h}\right) - \frac{1.8e^2}{\varepsilon r}$$

where E_g is the band gap of the bulk material (2.42 eV), $\hbar$ is the reduced Plank's constant (6.58×10^{-16} eV), r the radius of spherical nanocrystals, e is the charge of the electron (1.6×10^{-19} C), ε is the semiconductor dielectric constant (5.7), m_e and m_h are effective masses of the electrons and holes, respectively, and m_o is the free electron mass ($m_o = 9.11 \times 10^{-28}$ g). With the effective masses of electrons ($m_e = 0.19m_o$) and holes ($m_h = 0.8m_o$), diameters of 2.5, 2.7, 3.1, 3.5, and 3.9 ± 0.4 nm were found for CdS@MPA QDs obtained after 45 min, 1, 1.5, 2, and 3 h reaction, respectively. The deviation of

dx.doi.org/10.1021/am300232z | ACS Appl. Mater. Interfaces 2012, 4, 2561−2569

0.4 nm corresponds to ±10 nm for the determination of the absorption edges. The sizes of the CdS QDs were also estimated from the UV−vis absorption spectra by Peng's empirical equations[44] and were found to be in good accordance with results obtained from the Brus formula (2.3, 2.5, 2.9, 3.1, and 3.7 ± 0.4 nm for CdS@MPA QDs obtained after 45 min, 1, 1.5, 2, and 3 h reaction, respectively).

CdS nanocrystals prepared by the organometallic approach and its alternatives generally exhibit PL emission dominated by the band-edge emission.[44−47] Typically, for CdS QDs with diameters varying from 2.0 to 5.3 nm, the PL emission is located between 375 and 460 nm.[45] PL spectra of CdS@MPA nanocrystals corresponding to absorption spectra of Figure 2a are shown in Figure 2b. It can be seen that the PL peak position varies with heating time from 510 to 650 nm in a similar way as the absorption peak position and CdS nanoparticle diameter. The sizable difference between the emission peak position and the absorption edge indicates that the present CdS QDs exhibit trap-state emission rather than band-edge emission. The observed broad PL peak is commonly attributed to the recombination of charged carriers trapped in the surface states and is related to the size of CdS QDs.[48−51] The smaller the particles the more blue-shifted is the fluorescence band. In the CdS QDs prepared, the lack of stoichiometry for the chemical composition determined by EDS (vide infra) perhaps causes defects on the CdS QDs surfaces. PL QYs for the samples have been determined using the Rhodamine 6G standard in ethanol, reached values up to 20% for the sample prepared during 3 h and were independent of the excitation wavelength between 300 and 400 nm (see the photoluminescence excitation spectra in Figure S1 in the Supporting Information). PL QYs values increase continuously with increasing hydrothermal heating duration (10.9, 14.0, 14.5, 15.2 and 20.0% for 45 min, 1, 1.5, 2, and 3 h heating, respectively). Inset of Figure 2c shows digital photograph of MPA-capped CdS QDs which is consistent with the UV−vis and PL spectra data. This increasing PL QY with crystal growth for CdS QDs was also recently observed for CdS nanocrystals prepared in organic solvent.[52] It can also be seen that the full-width-at-half-maximum (fwhm) of PL emission spectra prepared through our method is ca. 110 nm, which is 3−4 times wider than the emission peaks of CdS QDs prepared in organic medium at elevated temperature.[44−47] This is typical of CdS QDs obtained through synthetic routes in aqueous media. Compared to aqueous syntheses of CdS QDs that use *meso*-2,3-dimercaptosuccinic acid,[53] thioglycolic acid or 3-mercaptopropanoic acid,[54,55] thioglycerol,[56] 2-mercaptoethanol,[57] dendrimers,[58] poly(vinyl alcohol),[59] or poly(acrylic acid)[60] as surface ligands, our method provides QDs with greater color tunability and higher PL QYs than those previously reported. Moreover, the shape of the PL band for our nanocrystals is also simpler, indicating particles with fewer defects. Finally, the time evolution of the optical properties of the as-prepared nanocrystal solutions after synthesis indicates highly reproducible behavior up to (at least) 4 months (see Figure S2 in the Supporting Information).

Concentration Effect. Figure 3 shows the evolution of the first excitonic peak of absorption spectra with growth at 100 °C when varying the concentration of $CdCl_2$ from 5 mM to 35 mM. In these reactions, the Cd^{2+}/thiourea/MPA molar ratio was kept constant at 1/1.7/2.3. As can be seen, the control of the size can be obtained by adjusting the $CdCl_2$ concentration. For the same growth time, a higher concentration of $CdCl_2$ resulted in a slower growth of CdS@MPA QDs. For example,

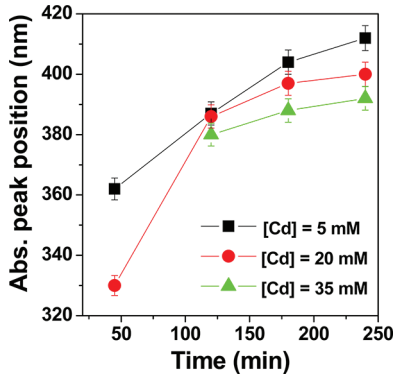

Figure 3. Evolution of the absorption peak position in function of reaction time at Cd^{2+} concentrations of 5, 20, and 35 mM.

when the reaction time was 180 min, the UV−vis absorption peaks of CdS QDs for concentration of $CdCl_2$ of 5, 20, and 35 mM were 404, 397, and 388 nm, respectively. The hydrothermal synthesis of CdS@MPA QDs follows classical La Mer behavior: higher precursor concentrations favor faster particle nucleation and slower growth, resulting in more numerous and smaller particles.[61]

When the concentration of $CdCl_2$ was 5 mM, the CdS QDs were synthesized with optimal optical properties, as evidenced by their well-defined absorption and good PL QYs (Figure 2). For example, CdS@MPA QDs obtained after 3 h heating at 100 °C have a PL QY of 20%. For the same growth time, the PL QY was decreased to 7.7 and 6.3% with increasing the concentration of $CdCl_2$ to 20 and 35 nm, respectively.

Influence of the Cd^{2+}/MPA Molar Ratio. Another series of experiments varied the concentration of MPA while holding the concentrations of $CdCl_2$ and thiourea constant and performing the reaction for 3 h at 100 °C. Figure S3 in the Supporting Information shows that as the ratio of MPA to Cd^{2+} + thiourea increases, the UV−vis absorption and PL emission spectra shift to the red, indicating the formation of larger CdS nanocrystallites with more surface defects than those prepared with smaller Cd^{2+}/MPA ratios (1/1.3 or 1/2.3). Meanwhile, the PL intensity showed a trend to increase first and decrease later, with maximum intensity at Cd^{2+}/MPA = 1/2.3. The PL QYs of CdS@MPA QDs prepared with Cd^{2+}/MPA ratios of 1/1.3, 1/2.3, and 1/4.5 were found to be 2.27, 20.0, and 1.05%, respectively. This can be explained by the fact that increasing the amount of MPA in solution leads to increasing MPA hydrolysis, and as a result, to a higher sulfide S^{2-} content in the reaction medium that accelerates the nanocrystals growth. It is also worthy to mention that for the lowest Cd^{2+}/MPA ratio (1/1.3), the dispersion stability was significantly lower and particles started to precipitate within one week. The reduced colloidal stability of these CdS@MPA QDs is probably a consequence of an incomplete surface passivation of the dots. Considering the need for strong light intensity for bioapplications and imaging, 1/2.3 was chosen as the best Cd^{2+}/MPA ratio in this study.

Effect of pH during the Synthesis. Figure 4 presents the evolution of the absorption and photoluminescence spectra of the as-prepared CdS nanocrystals grown for 3 h at three pH values (8, 10, and 12). As shown in Figure 4, the growth rate of MPA-capped CdS QDs is the quickest at pH 10 (excitonic peak λ_{abs} at ca. 403 nm and emission peak λ_{em} at 602 nm), the slowest at pH 8 (λ_{abs} = 372 nm, λ_{em} = 567 nm), whereas pH 12 was found to be intermediate (λ_{abs} = 389 nm, λ_{em} = 583 nm).

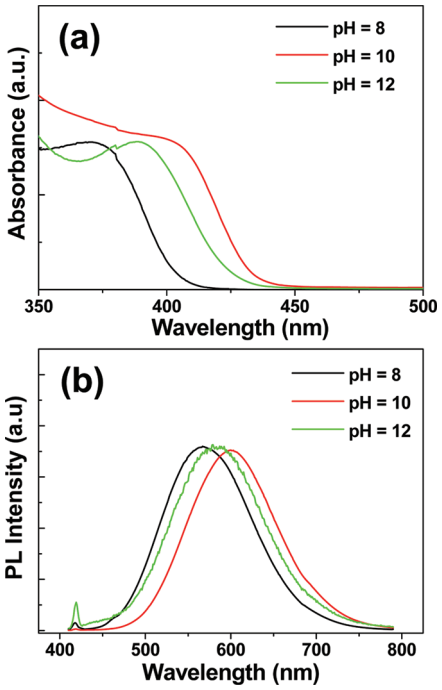

Figure 4. (a) UV–visible and (b) photoluminescence spectra of CdS@MPA QDs when varying the pH of the growth solution from 8 to 12. The reaction time was fixed to 3 h.

We also found that at the highest pH value, weak luminescence (PL QY = 2%) was obtained. The PL QY was increased with lowering of the pH of Cd^{2+}/thiourea precursors to 10 (PL QY = 14%). Further lowering of the pH to 8.0 led to a slight decrease in the photoluminescence of CdS@MPA QDs (PL QY = 12%). These pH-dependent effects could be attributed to decomposition kinetics of thiourea. At pH 12, S^{2-} is probably produced to quickly leading to CdS nanocrystals with more surface defects resulting in poor optical properties. The more gradual decomposition of thiourea at pH 8 or 10 producing HS^{-}, which needs a deprotonation step before the formation of CdS clusters, probably favors the homogeneous growth of CdS QDs.

XRD and TEM Studies. CdS QDs were further characterized by X-ray powder diffraction (XRD) and transmission electron microscopy (TEM). The XRD pattern of CdS@MPA QDs shows broad peaks indicating nanodimensions of the sample (Figure 5). Poor crystallinity was observed for the sample obtained after 45 min heating at 100 °C, which can be attributed to the short reaction time. With the increase of heating duration, peaks become more prominent and sharp due to the increase in nanocrystalline size. The peaks are positioned at 2θ = 26.5, 43.9, and 51.6°, oriented along the (111), (220), and (311) directions and are in good agreement with the JCPDS file 10–454, suggesting that the nanoparticles are in cubic zinc blende form.

TEM images of the CdS nanocrystallites prepared during 45 min, 1.5 and 3 h heating are shown in panels a-c of Figure 6, respectively. Insets of Figure 6a–c show the corresponding selected area electron diffraction (SAED) patterns for CdS@MPA QDs. Figure 6d–f confirms that the particle size of CdS QDs depends on the duration of the heating. The images show that CdS@MPA QDs are spherical, well-defined, and uniform in size. The diameters of the nanocrystals determined by TEM were 2.4 ± 0.4, 3.1 ± 0.4, and 3.5 ± 0.5 nm for 45 min, 1.5 h, and 3 h reaction, respectively. The average sizes obtained from UV–vis spectra and TEM matched each other reasonably well. A HR-TEM image of CdS@MPA QDs prepared for 3 h reaction is shown in Figure 7. As can be seen, the lattice planes of the CdS QDs are well resolved. From the lattice fringes of the micrograph, the interplanar spacing (d) was estimated to be 0.34 nm, which is correlated to the d value of (111) plane, i.e., 0.335 nm of the cubic phase. The cubic zinc blende structure of the produced CdS nanoparticles was further evidenced by the observation that a lattice spacing of 0.36 nm, which is found only the hexagonal phase, was not observed in any of our samples.

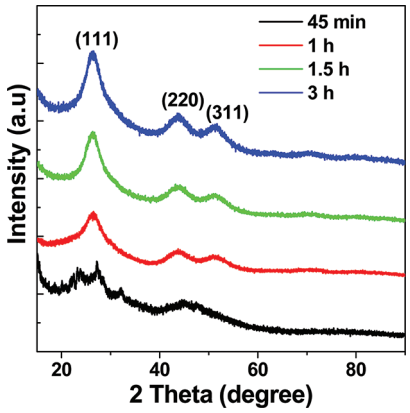

Figure 5. XRD patterns of the as-prepared CdS@MPA QDs as a function of heating time.

Figure 7b shows the EDS spectrum acquired from CdS@MPA QDs prepared via hydrothermal reaction for 3 h and confirms the chemical purity of the QDs. The calculated concentration ratio of the elements Cd and S is 0.71, which is acceptable against the exact value 1 and considering that S atoms are also present in the ligand.

Effect of pH on MPA-Capped CdS QDs PL. The PL efficiency of CdS nanocrystals was found to depend on the pH value of the colloidal solution. The variation of the fluorescence intensity under different pH values is shown in Figure 8 for yellow-emitting CdS@MPA QDs simply purified from the crude reaction mixture by precipitation and washing with ethanol. The PL QY was found to be 14% at pH 12. Upon addition of a 0.1 M HCl solution, the PL QY was found to be stable until neutrality, then it decreased drastically when the solution was adjusted into the acidic range and QDs start to aggregate. During this process, only decreases in absorption and PL intensity could be observed, indicating that the changes in pH influence the surface and not the size of the dots.

Cadmium can form complexes with thiourea,[62–64] sulfide, and hydrogenosulfide[65] produced by thiourea decomposition. The concentration of these complexes decreases as the pH of the solution decreases from a neutral to acidic range. These complexes can be considered as a wide bandgap material allowing exciton internalization and thus leading to an improvement in radiative recombination. It is therefore likely that the particle surface coverage with these complexes is strongly decreased at pH <7, thus increasing the number of trap sites and decreasing the PL QY.

This hypothesis was further supported by the experimental results obtained from dialyzed CdS QDs. The change of PL QY of the 4-h-dialyzed CdS QDs as function of pH is reported in Figure 8a. The PL QY of this sample decreased gradually from

dx.doi.org/10.1021/am300232z | ACS Appl. Mater. Interfaces 2012, 4, 2561–2569

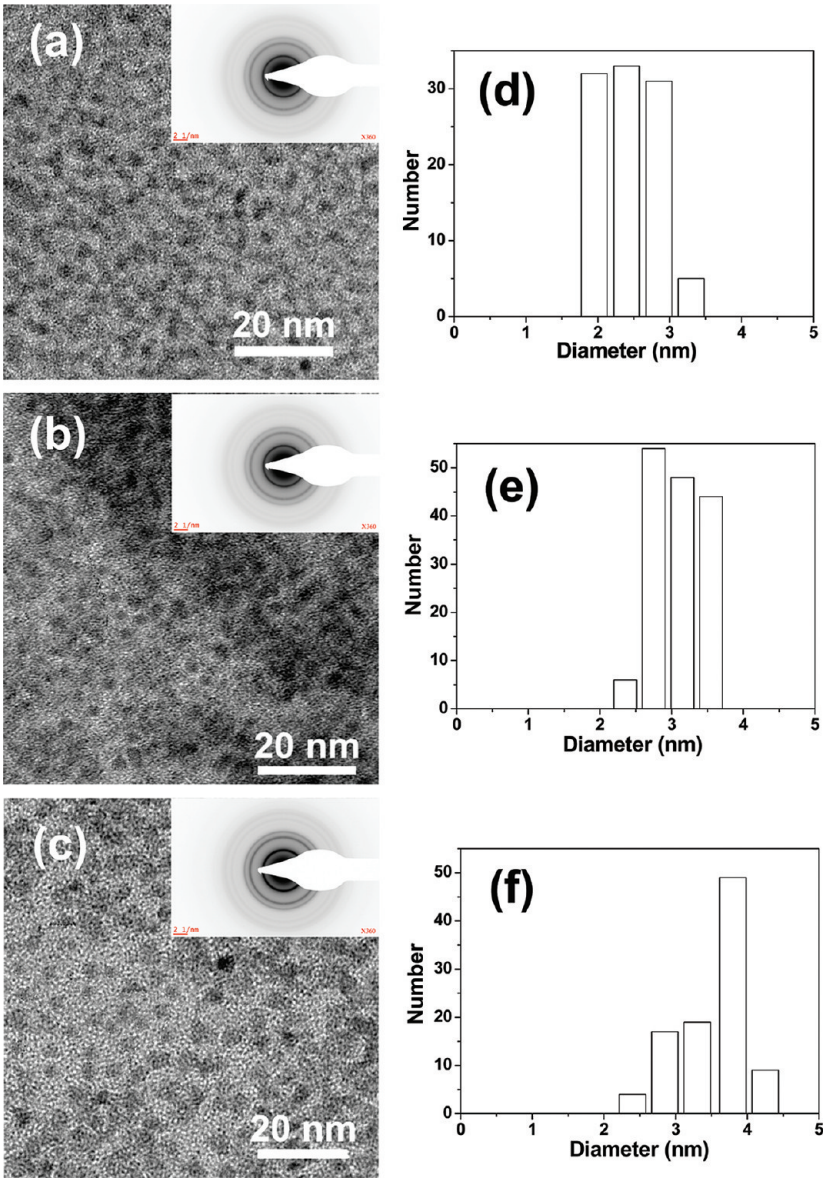

Figure 6. TEM images of CdS nanocrystallites prepared under hydrothermal conditions for (a) 45 min, (b) 1.5 h, and (c) 3 h. Insets show the SAED patterns. (d–f) Corresponding size distributions.

14 to 12% until pH 5 without significant changes in the shape or wavelength of the emission peak. Below pH 7, PL changes are markedly less pronounced than those observed for nondialyzed CdS@MPA QDs. A strong decrease of PL intensity is only observed below pH 5 and QDs start to precipitate at pH 4, probably due to the dissociation of the surface MPA ligands. This result demonstrates that the pH effect on PL intensity of the CdS QDs is related to Cd^{2+}-thiourea or Cd^{2+}-thiol complexes formed on the surface of QDs during the synthesis, because these species can be removed during dialysis from CdS cores.

Another evidence arises from matrix-assisted laser desorption/ionization using time-of-flight technique (MALDI-TOF) mass spectrometry data, which gives single high-intensity Gaussian-shaped peaks centered at m/z values of roughly 45 000 and 37 000 Da for CdS@MPA QDs before and after dialysis, respectively (Figure 8b), illustrating a decrease in size from 3.1 to 2.9 nm using the model of Inoue.[66] The comparison of the two spectra indicates the elimination of complexes with a mass of ca. 8000 Da during dialysis and confirms the attachment of polynuclear Cd-complexes at the surface of the dots after synthesis.

Epitaxial Growth of the ZnS Shell. In recent years, many efforts have been made to synthesize CdS/ZnS core/shell nanostructures.[67−71] Indeed, CdS and ZnS are II–VI group semiconductors, and they have similar crystalline structure (lattice mismatch of 6.4%). As ZnS is a phosphor material with a wide bandgap energy of 3.66 eV, passivation of CdS@MPA QDs surface with ZnS can greatly enhance the core properties. To prepare ZnS coated CdS QDs, a mixture of $Zn(OAc)_2$ and MPA was added to CdS@MPA QDs and the solution was heated at 100 °C for 4 h. Figure 9 presents typical UV–vis absorption and PL spectra of the original 3.1 nm-sized CdS cores and corresponding CdS/ZnS type-I QDs during the shell growth. No shift was observed for excitonic absorption peaks and for PL emission wavelengths (λ_{em} = 612 nm) but PL QYs increased gradually from 15 to 22% during the 4 h of heating and then reached a plateau. It is also worthy to note that the

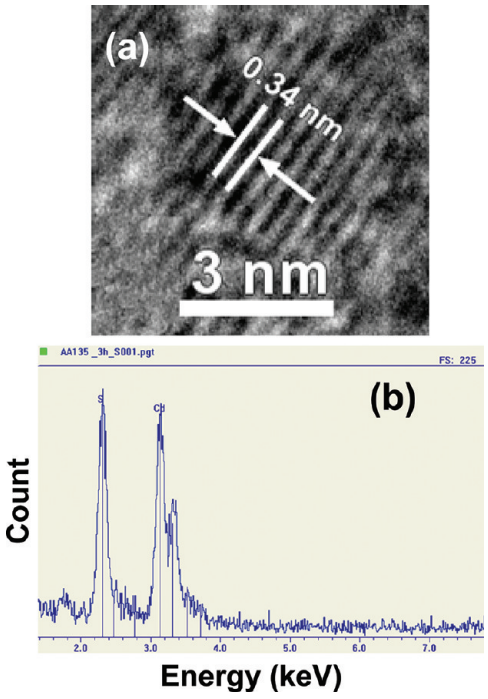

Figure 7. (a) HR-TEM image of CdS@MPA QDs prepared for 3 h at 100 °C with the emission at 650 nm. (b) Corresponding EDS spectrum.

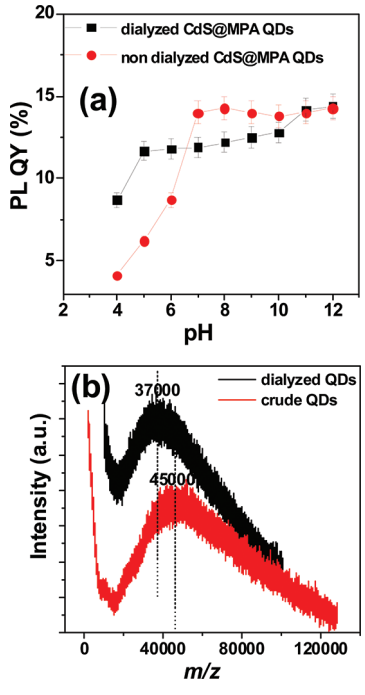

Figure 8. (a) Effect of pH on the PL QY of CdS@MPA QDs. (b) MALDI-TOF MS spectra of 3.1 nm-CdS@MPA QDs (estimated by TEM) before and after dialysis using dithranol as the matrix.

magnitude of the PL is clearly dependent on the core size with a larger PL increase for smaller QDs (PL QY increase from 20 to 23% for 3.5 nm-sized CdS QDs). Such an effect was also reported when growing a CdS shell around CdSe QDs.[72]

Figure 10a shows a TEM image of the as-prepared CdS/ZnS core/shell nanocrystals. In comparison to that of CdS QDs (3.1 nm), the size of CdS/ZnS nanocrystals increased to 3.6 nm,

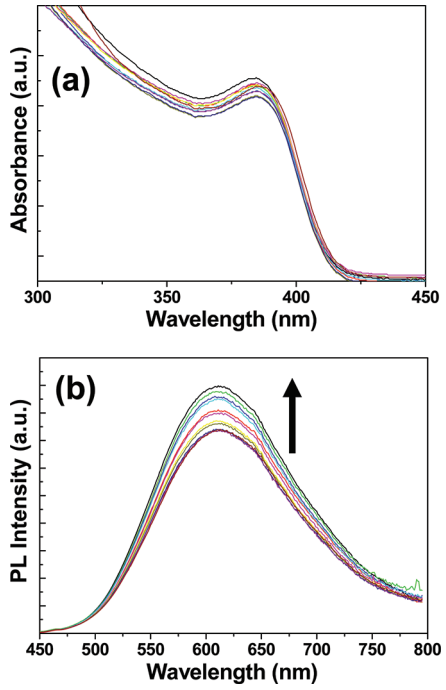

Figure 9. Evolution of (a) UV−vis absorption spectra and (b) PL emission spectra during the growth of the ZnS shell around 3.1 nm sized CdS cores. All spectra were recorded with an excitation wavelength of 400 nm.

which indicates an optimal thickness of 0.5 nm for the ZnS shell. The composition of the CdS/ZnS QDs was also investigated by EDS. In the EDS pattern, the presence of Zn was clearly confirmed, and the atomic ratio of Cd/S/Zn was calculated to be 10.7/13/1.2. HR-TEM micrograph of the core/shell QDs shows obvious lattice planes that extend across the entire particle with no evidence of an interface between the core and shell, which is consistent with a coherent epitaxial growth mechanism and demonstrates that the shell growth does not disturb the crystalline form of the core (Figure 10b). Figure 10c reveals the XRD pattern of original 3.1 nm-CdS cores and corresponding CdS/ZnS QDs. No separate peaks are observed, indicating clearly the formation of heterostructure.

Photostability Experiments. As shown in Figure S4 and S5 in the Supporting Information, the integrated PL intensities of 3.1 and 3.5 nm-sized CdS and of the corresponding CdS/ZnS QDs are stable and no aggregates are formed over the 30 min irradiation with a Hg−Xe lamp. For CdS QDs, the nanocrystal fluorescence increased during the first minutes of illumination and then leveled off at a constant value corresponding to 109−114% of the initial value. Although a very slight decline of PL intensity was observed upon irradiation of CdS/ZnS QDs, it still remained at 90−95% of its initial value after the 30 min irradiation. In both cases, no shift in absorbance and PL emission peaks were observed, thus confirming the good photostability of the dots (see Figures S6−S9 in the Supporting Information).

CONCLUSION

In summary, we have developed a one-pot noninjection hydrothermal route for producing good quality CdS QDs with a cubic structure from cadmium chloride and thiourea using mercaptopropionic acid as stabilizer. Various synthetic parameters, such as the initial Cd/thiourea/MPA ratio, the

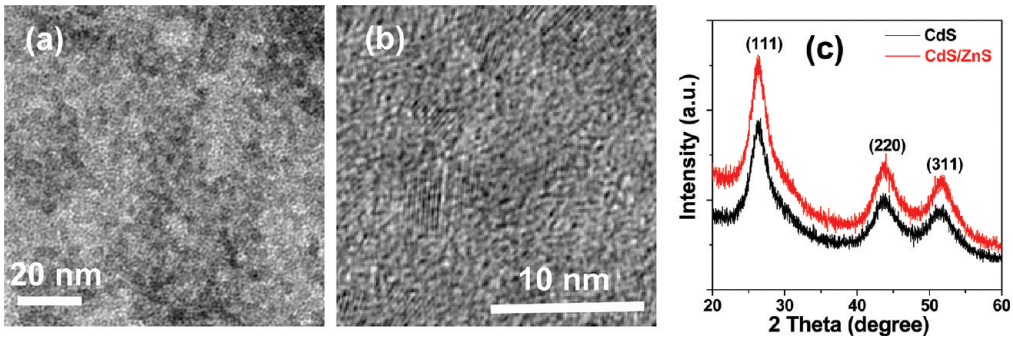

Figure 10. (a) TEM and (b) HR-TEM images of CdS/ZnS core/shell QDs, and (c) Powder X-ray diffraction patterns of CdS core QDs and CdS/ZnS core/shell QDs.

concentration of precursors, and the pH were found to affect the growth and the optical properties of CdS@MPA QDs. In optimal conditions, the emission wavelength of CdS QDs can shift from 510 to 650 nm in less than 3 h and the best PL QY can reach up to 20%. The combination of moderate pH value, low concentration of precursors and slow growth rate plays the crucial role in the good optical properties of the obtained CdS nanocrystals. Surface passivation of CdS@MPA cores by a wider bandgap material, ZnS, led to enhanced luminescence intensity (PL QY up to 23%). Because the colloidal solutions of CdS@MPA and CdS/ZnS QDs present very good photostability, the current investigation provides a useful synthetic route for producing water-dispersible and fluorescent CdS core nanocrystals that should easily be applicable in biology, optical coding, or optoelectronic devices. Work is under progress to broaden the synthetic protocol for additional QDs classes, such as alloyed QDs, and Cd-free doped dots like Mn^{2+}-doped ZnS.

■ ASSOCIATED CONTENT

Ⓢ Supporting Information

Further materials characterization and supporting figures described in the text. This material is available free of charge via the Internet at http://pubs.acs.org.

■ AUTHOR INFORMATION

Corresponding Author

*Phone: +33 3 83 17 50 53. E-mail: raphael.schneider@ensic.inpl-nancy.fr.

Notes

The authors declare no competing financial interest.

■ ACKNOWLEDGMENTS

We thank the Agence Nationale de la Recherche (ANR) for the financial support under contract ANR-09-JCJC-0029-01.

■ REFERENCES

(1) Kroutvar, M.; Ducommun, Y.; Heiss, D.; Bichler, M.; Schuh, D.; Abstreiter, G.; Finley, J. J. *Nature* **2004**, *432*, 81.
(2) Gao, X. H.; Cui, Y. Y.; Levenson, R. M.; Chung, L. W. K.; Nie, S. M. *Nat. Biotechnol.* **2004**, *22*, 969.
(3) Michalet, X.; Pinaud, F. F.; Bentolila, L. A.; Tsay, J. M.; Doose, S.; Li, J. J.; Sundaresan, G.; Wu, A. M.; Ghambir, S. S.; Weiss, S. *Science* **2005**, *307*, 538.
(4) Moussodia, R. -O.; Balan, L.; Merlin, C.; Mustin, C.; Schneider, R. *J. Mater. Chem.* **2010**, *20*, 1147.
(5) Aldeek, F.; Mustin, C.; Balan, L.; Roques-Carmes, T.; Fontaine-Aupart, M. -P.; Schneider, R. *Biomaterials* **2012**, *32*, 5459.
(6) Aboulaich, A.; Balan, L.; Ghanbaja, J.; Medjahdi, G.; Merlin, C.; Schneider, R. *Chem. Mater.* **2011**, *23*, 3706.
(7) Mc Clean, I. P.; Thomas, C. B. *Semicond. Sci. Technol.* **1992**, *7*, 1394.
(8) Weinhardt, L. *Appl. Phys. Lett.* **2003**, *82*, 571.
(9) Ouyang, J.; Kuijper, J.; Brot, S.; Kingston, D.; Wu, X.; Leek, D. M.; Hu, M. Z.; Ripmeester, J. A.; Yu, K. *J. Phys. Chem. C* **2009**, *113*, 7579.
(10) Li, H.; Shih, W. Y.; Shih, W. -H. *Ind. Eng. Chem. Res.* **2007**, *46*, 2013.
(11) Mansur, H. S.; Mansur, A. A. P.; Gonzales, J. C. *Polymer* **2011**, *52*, 1045.
(12) Vossmeyer, T.; Katsikas, L.; Giersig, M.; Popovic, I. G.; Diesner, K.; Chemseddine, A.; Eychmüller, A.; Weller, H. *J. Phys. Chem.* **1994**, *98*, 7665.
(13) Peng, Z. A.; Peng, X. *J. Am. Chem. Soc.* **2000**, *123*, 183.
(14) Zhong, X.; Feng, Y.; Knoll, W.; Han, M. *J. Am. Chem. Soc.* **2003**, *125*, 13559.
(15) Peng, X.; Wickham, J.; Alivisatos, A. P. *J. Am. Chem. Soc.* **1998**, *120*, 5343.
(16) Hines, M. A.; Guyot-Sionnest, P. *J. Phys. Chem. B* **1998**, *102*, 3655.
(17) Qu, L.; Peng, X. *J. Am. Chem. Soc.* **2002**, *124*, 2049.
(18) Sooklal, K.; Hanus, L. H.; Ploehn, H. J.; Murphy, C. J. *Adv. Mater.* **1998**, *10*, 1083.
(19) Winter, J. O.; Liu, T. Y.; Korgel, B. A.; Schmidt, C. E. *Adv. Mater.* **2001**, *13*, 1673.
(20) Barglik-Chory, C.; Remenyi, C.; Strohm, H.; Müller, G. *J. Phys. Chem. B* **2004**, *108*, 7637.
(21) Chen, S.; Zhu, J.; Shen, Y.; Hu, C.; Chen, L. *Langmuir* **2007**, *23*, 850.
(22) Celebi, S.; Erdamar, A. K.; Sennaroglu, A.; Kurt, A.; Acar, H. Y. *J. Phys. Chem. B* **2007**, *111*, 12668−12675.
(23) Thangadurai, P.; Balaji, S.; Manoharan, P. T. *Nanotechnology* **2008**, *19*, 435708.
(24) Pradhan, N.; Efrima, S. *J. Am. Chem. Soc.* **2003**, *125*, 2050.
(25) Cao, Y. C.; Wang, J. *J. Am. Chem. Soc.* **2004**, *126*, 14336.
(26) Yang, Y. A.; Wu, H.; Williams, K. R.; Cao, Y. C. *Angew. Chem., Int. Ed.* **2005**, *44*, 6712.
(27) Ouyang, J.; Vincent, M.; Kingston, D.; Descours, P.; Boivineau, T.; Zaman, M. B.; Wu, X.; Yu, K. *J. Phys. Chem. C* **2009**, *113*, 5193.
(28) Liao, L.; Zhang, H.; Zhong, X. *J. Lumin.* **2011**, *131*, 322.
(29) Govan, J. E.; Jan, E.; Querejata, A.; Kotov, N. A.; Gun'ko, Y. K. *Chem. Commun.* **2010**, *46*, 6072.
(30) Li, J.; Zhou, X.; Ni, S.; Wang, X. *Colloid J.* **2010**, *72*, 710.
(31) Karen, S.; Mallik, B. *J. Phys. Chem. C* **2007**, *111*, 16734.
(32) Grabolle, M.; Spiles, M.; Lesnyak, V.; Gaponik, N.; Eychmüller, A.; Resch-Genger, U. *Anal. Chem.* **2009**, *81*, 6285.
(33) Sahu, S. C.; Sahu, S. N. *Thin Solid Films* **1993**, *235*, 17.
(34) Froment, M.; Linvot, D. *Electrochim. Acta* **1995**, *40*, 1293.
(35) George, P. J.; Sa'nchez, A.; Huang, L. *J. Cryst. Growth* **1996**, *158*, 53.
(36) Brien, P.; O'Saeed, T. *J. Cryst. Growth* **1996**, *158*, 497.

(37) Mandal, P.; Talwar, S. S.; Major, S. S.; Srinivasa, R. S. *J. Chem. Phys.* **2008**, *128*, 114703.
(38) Matsumoto, H.; Sakata, T.; Mori, H.; Yoneyama, H. *J. Phys. Chem.* **1996**, *100*, 13781.
(39) Klimov, V. I. *J. Phys. Chem. B* **2000**, *104*, 6112.
(40) Moffitt, M.; Eisenberg, A. *Chem. Mater.* **1995**, *7*, 1178.
(41) Brus, L. E. *J. Chem. Phys.* **1984**, *80*, 4403.
(42) Wang, Y.; Herron, N. *J. Phys. Chem.* **1991**, *95*, 525.
(43) Henglein, A. *Chem. Rev.* **1989**, *89*, 1861.
(44) Yu, W. W.; Qu, L. H.; Guo, W. Z.; Peng, X. G. *Chem. Mater.* **2003**, *15*, 2854.
(45) Yu, W. W.; Peng, X. *Angew. Chem., Int. Ed.* **2002**, *41*, 2368.
(46) Pan, D.; Jiang, S.; An, L.; Jiang, B. *Adv. Mater.* **2004**, *16*, 982.
(47) Miao, Y.; Wu, Z.; Cao, L.; Fu, L.; He, Y.; Xie, S.; Zou, B. *Opt. Mater.* **2004**, *26*, 71.
(48) Fischer, C. -H.; Henglein, A. *J. Phys. Chem.* **1989**, *93*, 5578.
(49) Fujiwara, H.; Hosakawa, H.; Murakoshi, K.; Wada, Y.; Yanazida, S.; Okada, T.; Kobayashi, H. *J. Phys. Chem. B* **1997**, *101*, 8270.
(50) Diaz, D.; Rivera, M.; Ni, T.; Rodriguez, J. C.; Castillo-Blum, S. -E.; Nagesha, D.; Robles, J.; Alvarez-Fregoso, O. J.; Kotov, N. A. *J. Phys. Chem. B* **1999**, *103*, 9854.
(51) Carrot, G.; Scholz, S. M.; Plummer, C. J. G.; Hilborn, J. G.; Hedrick, J. L. *Chem. Mater.* **1999**, *11*, 3571.
(52) Chou, H. -L.; Tseng, C. -H.; Pillai, K. C.; Hwang, B. -J.; Chen, L. -Y. *J. Phys. Chem. C* **2011**, *115*, 20586.
(53) Sevinc, E.; Ertas, F. S.; Ulusay, G.; Ozen, C.; Acar, H. Y. *J. Mater. Chem.* **2012**, *22*, 5137.
(54) Zhou, R.; Wei, K.-Y.; Zhao, J.-S.; Jiang, Y.-B. *Chem. Commun.* **2011**, *47*, 6362.
(55) Wie, G.; Yan, M.; Ma, L.; Zhang, H. *Spectrochim. Acta A: Mol. Biomol. Spec.* **2012**, *85*, 288.
(56) Unni, C.; Philip, D.; Smitha, S. L.; Nissamudeen, K. M.; Gopchandran, K. G. *Spectrochim. Acta A: Mol. Biomol. Spec.* **2009**, *72*, 827.
(57) Chen, L.; Zhu, J.; Li, Q.; Chen, S.; Wang, Y. *Eur. Polym. J.* **2007**, *43*, 4593.
(58) Mansur, H. S.; Mansur, A. A. P.; Gonzalez, J. C. *Polymer* **2011**, *52*, 1045.
(59) Li, Q.; Cölfen, H.; Antonietti, M. *Nano Lett.* **2001**, *1*, 61.
(60) Lelebi, S.; Erdamav, A. K.; Sennaroglu, A.; Kurt, A.; Acar, H. Y. *J. Phys. Chem. B* **2007**, *111*, 12668.
(61) La Mer, V.; Dinegar, R. H. *J. Am. Chem. Soc.* **1950**, *72*, 4847.
(62) Ushasree, P. M.; Muralidharan, R.; Jayavel, R.; Ramasamy, P. *J. Cryst. Growth* **2000**, *218*, 365.
(63) Naumov, A. V.; Semenov, V. N.; Goncharaov, E. G. *Inorg. Mater.* **2001**, *37*, 647.
(64) Bao, N.; Shen, L.; Takata, T.; Domen, K.; Gupta, A.; Yanagisawa, K.; Grimes, C. A. *J. Phys. Chem. C* **2007**, *111*, 17527.
(65) Gao, M.; Kirstein, S.; Möhwald, H.; Rogach, A. L.; Kornowski, A.; Eychmüller, A.; Weller, H. *J. Phys. Chem. B* **1998**, *102*, 8360.
(66) Inoue, H.; Ichiroku, N.; Torimoto, T.; Sakata, T.; Mori, H.; Yoneyama, H. *Langmuir* **1994**, *10*, 4517.
(67) Hsu, Y. J.; Lu, S. Y. *Chem. Commun.* **2004**, 2102.
(68) Kar, S.; Santra, S.; Heinrich, H. *J. Phys. Chem. Lett.* **2008**, *112*, 4036.
(69) Kim, M. R.; Kang, Y. -M.; Jang, D. -J. *J. Phys. Chem. C* **2007**, *111*, 18507.
(70) Steckel, J. S.; Zimmer, J. P.; Coe-Sullivan, S.; Stott, N. E.; Bulovic, V.; Bawendi, M. G. *Angew. Chem., Int. Ed.* **2004**, *43*, 2154.
(71) Lu, S. -Y.; Wu, M. -L.; Chen, H. -L. *J. Appl. Phys.* **2003**, *93*, 5789.
(72) Mekis, A.; Talapin, D. V.; Kornowski, A.; Haase, M.; Weller, H. *J. Phys. Chem. B* **2003**, *107*, 7454.